Enhanced Magnetic Field Sensing Using Planar High-Temperature Superconductor Shields

J. Kvitkovic, S. Patel, M. Zhang, Z. Zhang, J. Peetz, A. Marney, and S. Pamidi, *Senior Member, IEEE*

***Abstract*—Experimental and finite element model studies of magnetic shielding characteristics of one-side planar sheet structures of the second generation high-temperature superconducting (2GHTS) coated conductor tapes show that significant shielding can be achieved. The shields are shown to be useful for attenuating noise and enhancing the measurement accuracy of magnetic fields. The shields are particularly important for shielding the perpendicular component of the noise during the measurements. The location of the sensor with respect to the shield and the dimensions of the shield need to be designed appropriately to achieve the needed measurement accuracy. The number of superconducting layers in the shield is a design parameter that depends on the magnitude of the noise. The experimental results on shielding factor of a single layer sheet agree with the results of the finite element model.**

***Index Terms*—Hall probe, magnetic field, magnetic shield, shielding factor, YBCO tape.**

I. Introduction

SHIELDING of magnetic field is necessary for many applications either to protect sensitive devices from external magnetic fields or to enhance the magnetic field measurements in a noisy environment. Shielding of magnetic field could be difficult to achieve depending on the magnitude, orientation, frequency, and special constraints of the magnetic field that needs to be shielded. If the frequency of the magnetic field source is high (> 1 MHz), highly conducting metals are used as shields by taking advantage of the skin effect. At low frequencies, magnetic screens made of conducting materials require large thickness to achieve required levels of attenuation, as the skin depth is large. For shielding of low frequency magnetic fields, soft ferromagnetic materials with very high relative permeability were utilized.

Planar magnetic shields were used in the medical electromagnetic tracking systems where metallic parts cause magnetic field distortions. Shielding is ideally done by completely surrounding the protected element, but if the element needs protection is large, a planar or one-side shield have to be used. Many ferromagnetic and conductive materials were explored at room temperature in a frequency range 1 Hz to 1 MHz. At lower frequencies, it is better to divert the flux lines using MuMetal or ferrite. At higher frequencies is advantageous to absorb or reflect the field using highly conductive materials such as copper [1].

Designing a one-side planar magnetic shield is particularly difficult because if the shield's dimensions are not large enough, magnetic field lines can flow through open paths. When the distance between the finite planar shield and source is long, the magnetic field will flow through the regions where there is no shield. This causes the shielding factor (SF) of the finite planar shield to be small. As the shield size decreases the magnetic field at the location of interest depends mainly on the magnetic field leakage around the edges of the shield. For open planar shields, the sensor position is critical for the evaluation of SF. Superconducting materials with their high conductivity are especially suited for fabricating magnetic shields [2].

If cryogenic coolant or cryocoolers are available, magnetic shields designed using high-temperature superconductors (HTS) have certain advantages. They allow lightweight and thinner structures useful for DC shielding as well as in a broad range of frequencies. Shields made of HTS materials allow high values of SF and hence are useful for magnetic shielding in many practical applications.

A superconducting magnetic shield made of two different superconducting HTS materials was studied by Tomkow [3]. The inner section was a bulk Bi-2223 cylinder, which provides complete shielding below its full penetration field. The outer section consists of rings formed of YBCO-123 tapes, which are capable of attenuating AC magnetic fields that reduce the magnetic field value on the inner bulk cylinder. By using the additional YBCO rings on a Bi-2223 bulk cylinder, the SF of the whole system was considerably increased from 17 % to 87 % at 33 Hz and 10 mT [3]. Tomkow also studied two shields each with eight YBCO rings with joint length 2 and 5 mm with resistances 2.6 and 1 mΩ, respectively. It was found that attenuation factors of YBCO rings can be enhanced by reducing the joint resistance [4].

Our previous magnetic shielding studies dealt with HTS shields in different geometries as sheets and coils at various field magnitudes, frequencies, and orientations [5] - [9].

In this paper, we discuss the results of the experiments using one-side planar shields of HTS YBCO material. The experi-

This work was supported by the Office of Naval Research through the Grant N00014-16-1-2984 and American Superconductor provided the superconducting material.

J. Kvitkovic, S. Patel, Z. Zhang, J. Peetz, A. Marney and S. Pamidi are with Center for Advanced Power Systems, Florida State University, Tallahassee, Florida 32310, USA (e-mail: kvitkovic@caps.fsu.edu, www.caps.fsu.edu)

M. Zhang is with University of Bath, Bath, UK (e-mail: M.Zhang2@bath.ac.uk)

S. Pamidi is with the Electrical and Computer Engineering Department of FAMU-FSU College of Engineering, Tallahassee, Florida, USA (e-mail: pamidi@caps.fsu.edu).

ments were performed to understand the configuration that provided the highest shielding factor and to see the benefit of adding additional layers on the shielding factor. We focused on reduction background magnetic field noise in the vicinity of a magnetic field sensor by using a one-side planar shield. The spectrum of the noise can vary from DC to several hundred Hz. A finite element model using COMSOL was created for the one-side planar shield at 50 Hz and the results were compared to that obtained in the measurements. To our knowledge, there are no previous studies in the literature on passive one-side planar HTS magnetic shields. The study described in the paper is to develop planar superconducting shields to eliminate or reduce the background fields emanating from the structures and electrical devices that would otherwise perturb the magnetic field that needs to be measured. It is often difficult or impossible to remove the structures and the electrical devices and the measurements have to achieve the magnetic field that would have been present in the absence of the structures.

II. Experimental

One-side planar sheets were made from commercial YBCO coated conductor tapes with 45 mm width. The shields were tested in DC and AC magnetic fields up to 400 Hz to study their magnetic shielding properties. All the measurements were performed at 77 K, in a liquid nitrogen bath.

The second generation HTS coated conductors produced as 45 mm wide ribbon used to fabricate the shields were procured from American Superconductor Corporation [10]. The manufacturing process for YBCO tapes involves Rolling Assisted Biaxially Textured NiW Substrates (RABiTS) with several layers of the buffer materials. The 1 µm layer of YBCO superconductor material was deposited using the metal oxide deposition (MOD) technology. The critical current of the 45 mm wide YBCO tape was higher than 1 kA at 77 K in the self-magnetic field. Fiber glass reinforced epoxy (G10) sheets were used for the support structure for the shields. The sample holder G10 plate had the dimensions of 60 mm x 120 mm, Fig. 1a. The superconducting ribbon was cut into sections of 45 mm x 100 mm and was attached to the support plate using Kapton tape. SF was measured as a function of magnetic field magnitude, the distance between the Hall probe (HP) sensor to shield, and the number of layers of superconducting tape in the shield. The gaps between the superconducting layers were kept to a minimum by using Kapton adhesive tape to attach the successive layers on the G10 support plate. The sample holder was inserted into the bore of helical copper magnet housed in a stainless steel cryostat, Fig. 1b. The cryostat was filled with liquid nitrogen. The helical copper magnet [11] produces a homogenous AC or DC magnetic field in the region of the superconducting shields. The external magnetic field was perpendicular to the wide plane of the shields. The copper magnet was supplied by the current from Techron AC/DC power supply that was controlled by an AC/DC function generator, Fig. 2. The magnet current was measured using a Hall probe current transducer. From magnet constant and current through the magnet, the magnitude of external magnetic field B_{ext} was calculated. For the experiments

FIG. 1, 2 HERE

with AC magnetic fields, a capacitor bank in a series resonance was used to compensate for the magnet inductance. There is a slight phase shift in the output current from the series resonance circuit compared to the excitation signal. The phase shift depends on the frequency. Hence the signal from the current transducer, instead of the excitation signal, was used. This technique was validated in our earlier phase sensitive measurements [15]. Before using the Hall probe in shielding experiments, it was calibrated at 77 K, for each frequency used. The calibration constants along with the measured Hall probe output voltage values were used to compute the value of the magnetic field at Hall probe location called B_{HP}, during the experiments with HTS shields. The magnetic field B_{HP} is the magnetic field that passed through the magnetic shields. The shielding factor *SF* was calculated using the B_{HP} and external magnetic field B_{ext} from the measurements by the following formula:

$$SF = \frac{B_{ext} - B_{HP}}{B_{ext}} * 100\ \% \qquad (1)$$

The B_{HP} was measured using a calibrated cryogenic Hall probe [12], which was perpendicular to external magnetic field vector. The center of the Hall probe was positioned at the geometric center of the sample. The sample and the sensor were placed in the center of the helical copper magnet, in the homogeneous magnetic field. An excitation current of 10 mA DC was supplied to the Hall probe by using a Lakeshore DC constant current source.

AC and DC signals were measured using voltmeters. For AC magnetic field the magnet current was measured by the Keithley 2001 multimeter. Hall probe voltage was measured using a lock-in amplifier. Before the beginning of each measurement, the frequency was set by the function generator. The reference signal for lock-in amplifier was derived from the Hall probe current transducer and amplified by the signal amplifier. For DC magnetic field measurements the Keithley 2001 multimeter was used as DC voltmeter. The current through the magnet and the Hall probe voltages were recorded for each measured point. This technique is scalable. The measurements described here were conducted using a double helix dipole magnet, but the same technique can be used for larger shields with any arbitrary source of the magnetic field generated by a single or multiple magnets as long as they are connected in series and powered by a single power supply.

III. 3D Finite Element Model

The 3D model represents the actual geometry of the 2GHTS tape with dimensions of 45 mm in width, 0.2 mm in thickness and 100 mm in length implemented in the finite element software COMSOL Multiphysics V5.3a. In the models, the YBCO layer and NiW substrate layer are considered, since the use of NiW ferromagnetic substrate changes the magnetic flux distribution in the region of the HTS tape [13]. Therefore, the model contains one air domain, one HTS subdomain, and one substrate subdomain. The model was developed based on the widely used

FIG. 3,4,5 HERE

H-formulation for electromagnetic diffusion [14]. Three partial differential equations as in equation (2), combining a set of Maxwell Equations in differential forms, are used as a governing equation for the entire three domains with dependent variables $\boldsymbol{H}$ [H_x, H_y, H_z]:

$$\mu_0\mu_r \frac{\partial \boldsymbol{H}}{\partial t} + \nabla \times (\rho \nabla \times \boldsymbol{H}) = 0 \qquad (2)$$

where μ_0 is the permeability of free space. The value of relative permeability μ_r of NiW substrate subdomain was obtained from measured values. The resistivity ρ of YBCO 2GHTS tape can be calculated by the E-J power law in the equation:

$$\rho = E_0[\frac{1}{J_{norm}}(\frac{J_{norm}}{J_c(B)})^n] \qquad (3)$$

where $J_{norm} = \sqrt{J_x^2 + J_y^2 + J_z^2}$. The magnetic field dependent critical current density $J_c(B)$ is considered, which is incorporated by interpolation of the measurement values studied in [15]. The electrical field criterion $E_0 = 1\mu V/cm$ and $n = 31$ are typical values used for YBCO tape. The resistivity ρ of the non-superconducting subdomains are constants and defined by Ohm's law, $\rho = E/J$. In order to simulate external AC magnetic field, the Dirichlet boundary condition was used in the air domain:

$$H_y = B_{ext}/\mu_0 \sin(2\pi f t) \qquad (4)$$

where the B_{ext} is the amplitude of AC magnetic field along the y direction (perpendicular to the wide tape face) with the frequency of 50 Hz.

IV. Results

DC shielding factor for 1 - 9 layer of the one-side planar shield at 77 K, at a distance of 7 mm from the Hall probe is presented in Fig. 3. At low magnetic field amplitudes (≤ 10 mT), the DC shielding factor is > 60 % for 3-9 layer shield. At higher magnetic fields > 50 mT, DC SF is dropping to 50 – 60 %. Shields with 8 and 9-layers have almost the same SF(B) dependence. SF(B) curves for 1 and 2-layer shields have different behavior, in field interval 10 – 20 mT they dropped with a slope 1%/mT. At low magnetic fields as more layers are added, the SF is increased. With increasing the magnetic field, the SF decreases. The curve starting with the highest shielding factor stays with the highest SF at higher magnetic fields, and the curve with the lowest SF stays with the lowest SF at the end of magnetic field interval.

Fig. 4 depicts the AC shielding factor of a nine-layer one-side planar shield as a function of AC magnetic field at 77 K, at 20 – 400 Hz, at a 5 mm distance from the Hall probe. Measured SF at 400 Hz was the highest (82 %) throughout the range of magnetic field up to 30 mT. For the higher magnetic field (> 30 mT) at frequencies 200 – 400 Hz, SF has started to drop to 30 – 50 %. SF at all other frequencies 20 – 100 Hz keeps quite constant at 65 – 70 % level.

FIG. 6,7,8 HERE

Fig. 5 shows magnetic field dependence of the SF at frequency 20 Hz for 1 – 9 layer one-side planar shield at 77 K in 4 – 50 mT magnetic field range, at a distance of 5 mm from the Hall probe. SF at 20 Hz has a similar SF(B) dependence as seen for DC. There is a correlation between the number of layers and the value of shielding factor. The greater the number of layers the higher the magnetic shielding. Single layer shield has a steady drop rate where the magnitude of SF drops quite steadily throughout the range of the magnetic field while the shields with ≥ 2 layers have a steady decrease rate and at 30 mT the rate of decrease increases. Even though the rate of decrease 2- and 3-layer shields increases after certain magnetic field the drop is not as steep as in the single-layer shield. The shielding factor stayed constant at ~ 67 % up to 30 mT for the 8 and 9 layer shields.

In Fig. 6 is plotted SF for the one-side planar shield as the function the distance between the shield and the Hall probe at 20 Hz and magnetic field of 21 mT for shields with 1 - 4 layers. The measured shielding factor is higher at locations that are closer to shield, and as one moves away from the shield the measured SF decreases. It was observed that the optimum superconductor to HP distance is 2 mm. The measured magnetic field results from two components: external magnetic field and the magnetic field generated by the magnetization currents in the superconductor. If we are too close to superconductor (0.3 mm) we are measuring the magnetic field generated by the superconductor. It was confirmed from the measurements while the external magnetic field is turned off.

Fig.7 shows a bar graph of the SF as a function of the number of layers at 4 mT for frequency 20, 100, 400 Hz. There are some fluctuations in the SF as the number of layers is increased. At all measured frequencies, a drop in SF was observed for the shields with 4 and 7 layers. It could be caused by superconductor interference with the ferromagnetic substrate, as the HTS is not perfectly flat and some local gaps between the layers could not be avoided.

When magnetic shields are exposed to perpendicular AC magnetic field, screening currents are induced in the region of HTS layer. A magnetic field probe was placed above the center of the HTS tape in the 3D model to measure the magnetic field at various distances 2, 5, and 15 mm from the HTS tape. Fig. 8 depicts the comparison between the simulated and experimental SF as a function of the external magnetic field. The model results show that the shielding factor decreases with increasing external magnetic field and with distance to the HTS layer, which is consisted with the trend observed in the experiments.

V. Conclusion

The design of a new apparatus for characterizing magnetic shielding properties of high-temperature superconductor in the form of one-side planar shields is presented. Shields were fabricated with up to 9 layers of the superconductor in sheet geometry using 45 mm wide commercial YBCO coated conductor tape. Shielding factors > 80 % were achieved at the magnetic field of 30 mT and frequency of 400 Hz at 77 K. Interesting

differences in frequency dependence of shielding factors were observed. The shielding factors increase with increasing frequency at the low external magnetic field and decrease with increasing frequency at high (> 40 mT) magnetic fields. Finite element model using COMSOL was used for AC shielding factor calculations for one layer sheet at 50 Hz at distances 2, 5, 15 mm from the sensor. The successful demonstration of high values, > 80 %, of shielding factors suggests that lightweight and thin magnetic shields could be prepared from several layers of commercial 2GHTS tapes for various applications. The superconducting shield, if designed appropriately, will eliminate the noise and allows the measurement of the unperturbed magnetic field.

REFERENCES

[1] K. O'Donoghue and P. Cantillon-Murphy, "Planar Magnetic Shielding for Use With Electromagnetic Tracking Systems," *IEEE Trans. on Magnetics*, vol. 51, no. 2, pp. 1-12, Feb. 2015 doi: 10.1109/TMAG.2014.2352344.

[2] L. Hasselgren and J. Luomi, "Geometrical aspects of magnetic shielding at extremely low frequencies," *IEEE Transactions on Electromagnetic Compatibility*, vol. 37, no. 3, pp. 409-420, Aug 1995 doi: 10.1109/15.406530.

[3] L. Tomków, M. Ciszek, and M. Chorowski, "Combined magnetic screen made of Bi-2223 bulk cylinder and YBCO tape rings—Modeling and Experiments," *Journal of Appl. Phys*. 117, 043901, 2015.

[4] L. Tomków, M. Ciszek, and M. Chorowski, "Frequency Effect on Shielding Quality of Closed Superconducting Magnetic Shields Made of Superconducting Tapes," *IEEE Trans. Appl. Supercond.*, Vol. 26, No. 3, April 2016.

[5] J. Kvitkovic, J. Voccio, and S. V. Pamidi, "Shielding of AC magnetic fields by coils and sheets of superconducting Tapes," *IEEE Trans. Appl. Supercond*., vol. 19, pp. 3577-3580, Jun. 2009.

[6] J. Kvitkovic, S. Pamidi, and J. Voccio, "Shielding AC magnetic fields using commercial $YBa_2Cu_3O_7$-coated conductor tapes," *Supercond. Sci. Technol*., vol. 22, no. 12, p. 125009, Oct. 2009.

[7] J. Kvitkovic, P. Patil, S. V. Pamidi, and J. Voccio, "Characterization of 2G superconductor magnetic shields at 40–77 K," *IEEE Trans. Appl. Supercond*., vol. 21, no. 3, pp. 1477-1480, Jun. 2011.

[8] J. Kvitkovic, D. Davis, M. Zhang, and S. Pamidi, "Influence of interlayer separation on magnetic shielding properties of 2G HTS sheets made of 46 mm wide RABiTS tape," *IEEE Trans. Appl. Supercond*., vol. 23, no. 3, pp. 8200605-8200605, Jun. 2013, Art. ID. 8200605.

[9] J. Kvitkovic, D. Davis, and M. Zhang, "Magnetic Shielding characteristics of second generation high temperature superconductors at variable temperatures obtained by cryogenic helium gas circulation," *IEEE Trans. Appl. Supercond.*, vol. 25, no. 3, pp. 1-4, Jun. 2015, Art. ID. 8800304.

[10] www.amsc.com

[11] www.advancemag.com

[12] www.arepoc.sk

[13] M. D. Ainslie, T. J. Flack, and A. M. Campbell, "Calculating transport AC losses in stacks of high temperature superconductor coated conductors with magnetic substrates using FEM" *Physica C: Supercond*., 2012, 472 (1), pp.50-56.

[14] M. Zhang, and T. A. Coombs, "3D modeling of high-Tc superconductors by finite element software" *Supercond. Science and Tech.* 2011, 25(1), p.015009.

[15] M. Zhang, J. Kvitkovic, J. H. Kim, C. H. Kim, S. Pamidi, and T. A. Coombs, "Alternating current loss of second-generation high-temperature superconducting coils with magnetic and non-magnetic substrate" *Applied Physics Letters*, 2012, 101(10), p.102602.

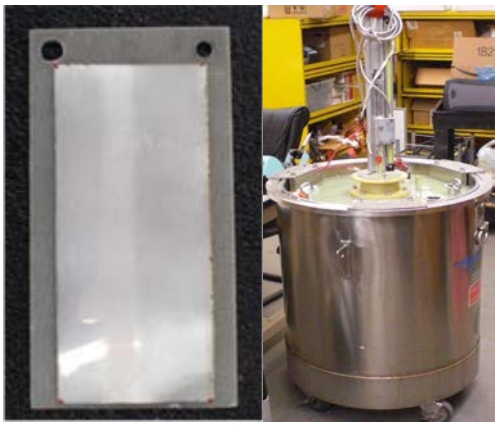

Fig. 1. Photographs of the sample a) and the magnet b) used for SF measurements.

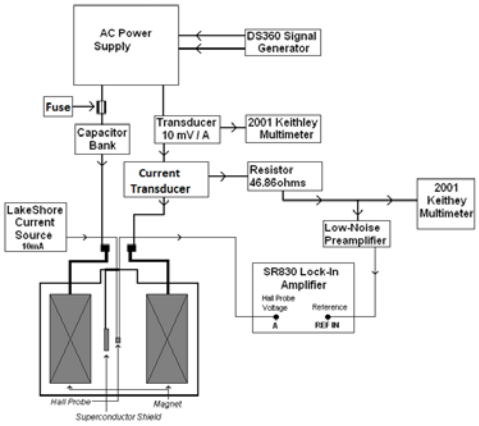

Fig. 2. A schematic of the experimental set-up for AC shielding measurements with one side planar sheets.

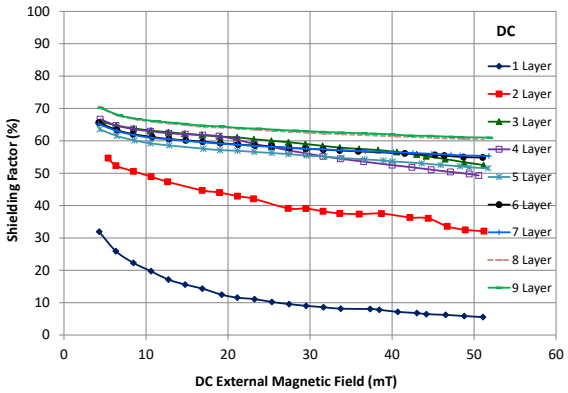

Fig. 3. DC shielding factor for 1 up to 9-layer one-side planar shield at 77 K.

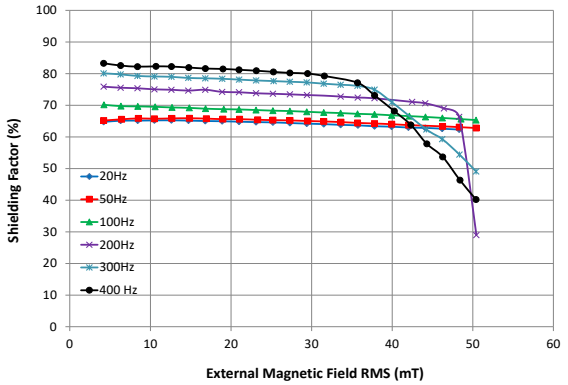

Fig. 4. AC shielding factor of a nine-layer one-side planar shield as a function of AC magnetic field at 77 K.

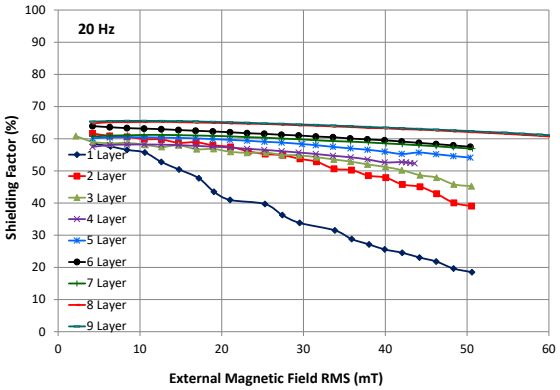

Fig. 5. AC shielding factor for 1 up to 9-layer one-side planar shield at 20 Hz.

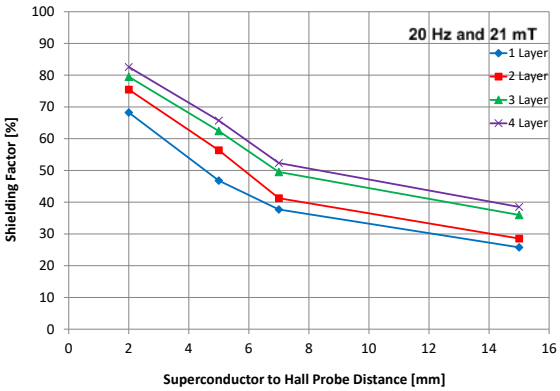

Fig. 6. Shielding factor as function of shield to Hall probe distance at 20 Hz and 21 mT for 1 up to 4-layer one-side planar shield.

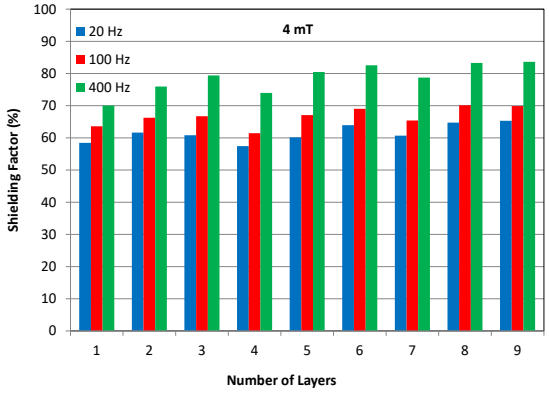

Fig. 7. Shielding factor as a function of number of layers at 4 mT for 20, 100, 400 Hz at 77 K.

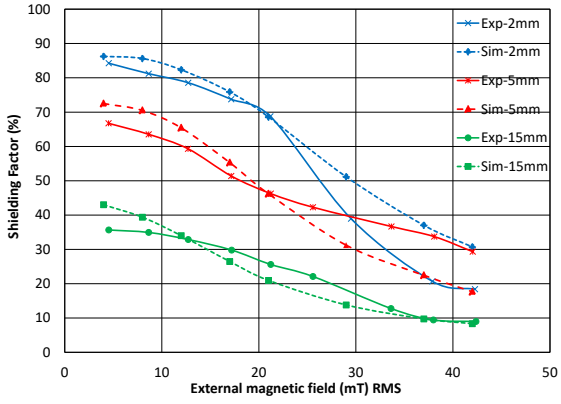

Fig. 8. Comparison of 3D simulation and experimental results of SF for the one-layer one-side planar shield at various distances 2, 5, 15 mm from the sensor at 50 Hz.